

Density Discontinuity of a Neutron Star and Gravitational Waves

Hajime Sotani¹ *, Kazuhiro Tominaga¹ †, and Kei-ichi Maeda^{1,2} ‡

¹ *Department of Physics, Waseda University, 3-4-1 Okubo, Shinjuku, Tokyo 169-8555, Japan*

² *Advanced Research Institute for Science and Engineering,
Waseda University, Shinjuku, Tokyo 169-8555, Japan*

(October 30, 2018)

We calculate quasi-normal f- and g-modes of a neutron star with density discontinuity, which may appear in a phase transition at extreme high density. We find that discontinuity will reflect largely on the f-mode, and that the g-mode could also be important for a less massive star.

PACS number(s): 04.25.Nx, 04.30.-w, 04.40.Dg

I. INTRODUCTION

Gravitational wave interferometers such as LIGO, VIRGO, GEO600, and TAMA300 on earth, and LISA in space [1] are almost ready to observe directly the gravitational waves from the Universe. The significance of direct observation of gravitational waves is that we obtain new method to observe the Universe by gravitational waves (the so-called gravitational wave astronomy), and that we may be able to verify the theory of gravity, and that new physics at high density or high energy region can be found by observing a merger of a binary neutron star.

The one of the sources of the gravitational waves is supposed to be supernova explosion, which occurs at the last phase of a massive star. After explosion, a newly formed compact object may oscillate violently, and the emitted gravitational waves carry the information of the sources. The oscillation will eventually damp out because that the gravitational waves carry the energy. The merger of two coalescing black holes or neutron stars is another source. It is naturally expected that the final object will also oscillate. If a final compact object is a neutron star, its structure will reflect on the emitted gravitational waves. There should be some relation between a structure of a neutron star and the emitted gravitational waves. The structure of a neutron star not yet well-known because the equation of state is uncertain at the high density over the nuclear density. Therefore, although main composition of matter in a neutron star is neutron, it is possible that there appear new phase in extremely high density such as a pion condensation, or a kaon condensation. In such a situation, a phase transition may occur, and if it is strongly first order, one may expect that there appears the discontinuity of density at some density as the case of the kaon condensation [2]. If we know in advance the relation between the structure of a neutron star and the emitted gravitational waves, we will get the information or the restriction on the equation of state over the nuclear density. In particular, if we find any specific feature in the emitted gravitational waves from a neutron star with discontinuity, we may be able to predict the existence of a phase transition in a neutron star. This is the main subject of the present paper. We will just focus into quasi-normal modes of a neutron star.

Although the gravitational waves emitted in a super-

nova explosion or from a merger of a binary may show very complicated wave form, only quasi-normal modes will eventually remain. We expect that these quasi normal modes contain a lot of information about a neutron star. Hence, it is very important for us to study those modes for a possible situation. The quasi normal modes are classified into various types. For the modes coupled to the fluid of a non-rotating neutron star, we have f-, p- and g-modes.

The damping rate of these modes is very small compared with the oscillation period of fluid because matter couples to gravity very weakly. There exists only one f-mode for each l . The p-mode which is caused by the pressure of fluid. The g-mode is originated by density discontinuity or temperature of a star. Its damping rate is usually quite small, so few calculation has been done. There also exists another mode (the so-called w-mode) which is related to metric perturbations of spacetime rather than fluid oscillation. This mode has high damping rate in comparison with modes related to fluid oscillation.

For the case without density discontinuity, the relation between quasi normal modes of a star and equation of state has been studied by many authors [3], [4], [5]. For g-mode, there are a few works. Newtonian case is studied in [6] and also in [10], which includes the effect of temperature of neutron stars by use of the Cowling approximation [9]. For the relativistic case, Finn adopted an approximate method which is called the “slow motion formalism” and calculated the imaginary part by the energy loss for the case of density discontinuity [7], [8].

Although these works are very important, they have not discussed density discontinuity at high density, which may appear via a phase transition. In this paper, we shall study a neutron star with such a discontinuity, and investigate its quasi normal modes. Just for simplicity, we assume that equation of state is given by a polytrope ($P = K\rho^{1+1/n}$). We discuss only even parity modes, which are coupled to oscillation of matter fluid in a neutron star. We then assume that there exists density discontinuity due to a phase transition and density discontinuity.

First we present the basic equations to solve in §II, including the equation for a background neutron star with density discontinuity. In §III, we show an explicit struc-

ture of a neutron star with the density discontinuity and numerical results for quasi normal modes. We also compare our results with those obtained by the relativistic Cowling approximation [11]. Conclusion is given in §IV. In Appendix A, we present the explicit boundary condition at the center of a star. In Appendix B, we briefly summarize the method of how to calculate the quasi normal modes.

In this paper we adopt the unit of $c = G = 1$, where c and G denote the speed of light and the gravitational constant, respectively, and the metric signature of $(-, +, +, +)$.

II. BASIC EQUATION

A. stellar model with discontinuity

We first construct a neutron star model with discontinuity of density to calculate its quasi-normal modes. A static and spherically symmetric spacetime is described by

$$ds^2 = -e^{2\Phi} dt^2 + e^{2\Lambda} dr^2 + r^2 (d\theta^2 + \sin^2 \theta d\phi^2), \quad (2.1)$$

where Φ, Λ are metric functions with respect to r . A mass function $m(r)$, which is defined as

$$m(r) = \frac{1}{2} r (1 - e^{-2\Lambda}), \quad (2.2)$$

satisfies

$$\frac{dm}{dr} = 4\pi r^2 \rho. \quad (2.3)$$

The equilibrium condition of a stellar model is given by the Tolman-Oppenheimer-Volkoff equation,

$$\frac{dP}{dr} = -\frac{(\rho + P)(m + 4\pi r^3 P)}{r(r - 2m)}, \quad (2.4)$$

where the function ρ and P are the energy density and the pressure of the fluid. The potential Φ is given by

$$\frac{d\Phi}{dr} = \frac{(m + 4\pi r^3 P)}{r(r - 2m)}. \quad (2.5)$$

With an additional equation, i.e. the equation of state, we can solve these equations.

As for the boundary conditions, there are two boundaries; the center of a star and the surface. The stellar radius R is determined by the condition that the pressure vanishes at the surface, i.e. $P(R) = 0$. The total mass M is given by $m(R)$, and the potential $\Phi(r)$ is smoothly connected at the surface, i.e.

$$e^{2\Phi(R)} = 1 - \frac{2M}{R}. \quad (2.6)$$

At the center, a regularity condition should be imposed.

As for the equation of state, just for simplicity, we adopt a polytropic equation of state except at a discontinuous surface of density, which is assumed to exist inside of the star. Then, the equation of state is given by two equations;

$$P = K_{(+)} \rho^{1+1/n_{(+)}} \quad \text{for } 0 \leq r \leq R_{\text{dis}}, \quad (2.7)$$

$$P = K_{(-)} \rho^{1+1/n_{(-)}} \quad \text{for } R_{\text{dis}} \leq r \leq R, \quad (2.8)$$

where R_{dis} is the radius of a discontinuous surface. The values of two adiabatic indices ($n_{(+)}$ and $n_{(-)}$), and those of two coefficients ($K_{(+)}$ and $K_{(-)}$) may be different. However, since the pressure should be continuous at the discontinuous surface R_{dis} , we have one constraint on those parameters. For example, $K_{(+)}$ is fixed as

$$K_{(+)} = K_{(-)} \times \frac{(\rho_{\text{dis}}^{(-)})^{[1+1/n_{(-)}]}}{(\rho_{\text{dis}}^{(+)})^{[1+1/n_{(+)}]}}. \quad (2.9)$$

Now we have six parameters; the central density of the star ρ_c , the inner density at the discontinuous surface $\rho_{\text{dis}}^{(+)}$, the ratio of the outer density to the inner density at the discontinuous surface $\rho_{\text{dis}}^{(-)}/\rho_{\text{dis}}^{(+)}$, the inner polytropic index $n_{(+)}$, the outer polytropic index $n_{(-)}$ and the outer polytropic coefficient $K_{(-)}$. Some examples of this equation of state with discontinuous density are given in Figure 1.

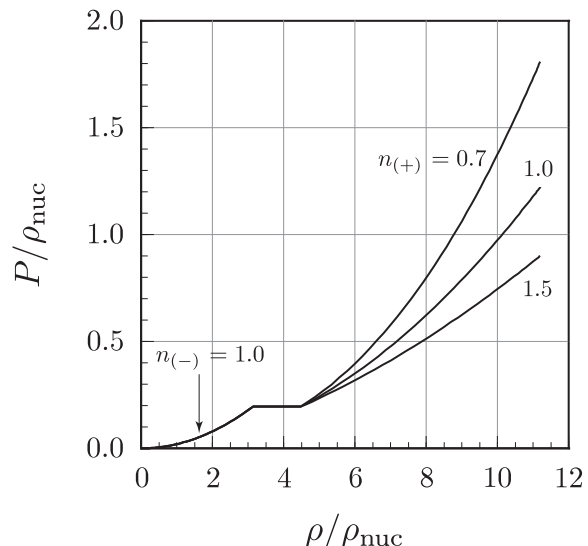


FIG. 1. Equation of state with density discontinuity. The density and pressure are normalized by the standard nuclear density $\rho_{\text{nuc}} = 2.68 \times 10^{14} \text{ (g/cm}^3\text{)}$. We set $\rho_c = 3.0 \times 10^{15} \text{ (g/cm}^3\text{)}$, $\rho_{\text{dis}}^{(+)} = 1.2 \times 10^{15} \text{ (g/cm}^3\text{)}$, $\rho_{\text{dis}}^{(-)}/\rho_{\text{dis}}^{(+)} = 0.7$, $K_{(-)} = 100 \text{ (km}^2\text{)}$ and $n_{(-)} = 1.0$.

B. perturbation equations inside the star

Here we present the basic equations for perturbations against the background metric of a spherically symmetric star (2.1). The perturbation is given by

$$g_{\mu\nu} = g_{\mu\nu}^{(B)} + h_{\mu\nu}. \quad (2.10)$$

The perturbations against a spherical background can be decomposed by the spherical harmonics Y_m^l , and are classified into two by its parity, i.e. odd or even. Because we are interested in to discuss relation between a discontinuity in stellar density and the gravitational waves emitted from such a neutron star, in this paper, we only study even-parity perturbations, in which gravitational waves are coupled to fluid oscillation.

Following the method by Lindblom and Detweiler [12], $h_{\mu\nu}$ is described as

$$h_{\mu\nu} = \begin{pmatrix} r^l \hat{H} e^{2\Phi} & i\omega r^{l+1} \hat{H}_1 & 0 & 0 \\ i\omega r^{l+1} \hat{H}_1 & r^l \hat{H} e^{2\Lambda} & 0 & 0 \\ 0 & 0 & r^{l+2} \hat{K} & 0 \\ 0 & 0 & 0 & r^{l+2} \hat{K} \sin^2 \theta \end{pmatrix} Y_m^l e^{i\omega t}, \quad (2.11)$$

where \hat{H} , \hat{H}_1 , and \hat{K} are the perturbed metric function with respect to r . The fluid perturbations are described by the Lagrangian displacement vectors $\xi^i = (\xi^r, \xi^\theta, \xi^\phi)$ as follows:

$$\xi^r = \frac{r^l}{r} e^\Lambda \hat{W} Y_m^l e^{i\omega t}, \quad (2.12)$$

$$\xi^\theta = -\frac{r^l}{r^2} e^\Lambda \hat{V} \frac{\partial}{\partial \theta} Y_m^l e^{i\omega t}, \quad (2.13)$$

$$\xi^\phi = -\frac{r^l}{r^2 \sin^2 \theta} e^\Lambda \hat{V} \frac{\partial}{\partial \phi} Y_m^l e^{i\omega t}, \quad (2.14)$$

where \hat{W} and \hat{V} are functions with respect to r . Furthermore we introduce the new variable \hat{X} instead of \hat{V} to make the boundary condition at the surface of a star simple (see below);

$$\hat{X} \equiv \omega^2 (P + \rho) e^{-\Phi} \hat{V} - \frac{e^{\Phi-\Lambda}}{r} \frac{dP}{dr} \hat{W} - \frac{1}{2} (P + \rho) e^\Phi \hat{H}. \quad (2.15)$$

The perturbation equations of the Einstein equations are given by

$$\begin{aligned} \frac{d\hat{H}_1}{dr} &= -\frac{1}{r} \left[l + 1 + \frac{2m}{r} e^{2\Lambda} + 4\pi r^2 (P - \rho) e^{2\Lambda} \right] \hat{H}_1 \\ &\quad + \frac{1}{r} e^{2\Lambda} \left[\hat{H} + \hat{K} + 16\pi (P + \rho) \hat{V} \right], \end{aligned} \quad (2.16)$$

$$\frac{d\hat{K}}{dr} = \frac{l(l+1)}{2r} \hat{H}_1 + \frac{1}{r} \hat{H} - \left(\frac{l+1}{r} - \frac{d\Phi}{dr} \right) \hat{K} + \frac{8\pi}{r} (P + \rho) e^\Lambda \hat{W}, \quad (2.17)$$

$$\frac{d\hat{W}}{dr} = -\frac{l+1}{r} \hat{W} + r e^\Lambda \left[\frac{1}{\gamma P} e^{-\Phi} \hat{X} - \frac{l(l+1)}{r^2} \hat{V} - \frac{1}{2} \hat{H} - \hat{K} \right], \quad (2.18)$$

$$\begin{aligned} \frac{d\hat{X}}{dr} &= -\frac{l}{r} \hat{X} + (P + \rho) e^\Phi \left[\frac{1}{2} \left(\frac{d\Phi}{dr} - \frac{1}{r} \right) \hat{H} - \frac{1}{2} \left(\omega^2 r e^{-2\Phi} + \frac{l(l+1)}{2r} \right) \hat{H}_1 \right. \\ &\quad \left. + \left(\frac{1}{2r} - \frac{3}{2} \frac{d\Phi}{dr} \right) \hat{K} - \frac{l(l+1)}{r^2} \frac{d\Phi}{dr} \hat{V} \right. \\ &\quad \left. - \frac{1}{r} \left(\omega^2 e^{-2\Phi+\Lambda} + 4\pi (P + \rho) e^\Lambda - r^2 \left\{ \frac{d}{dr} \left(\frac{1}{r^2} e^{-\Lambda} \frac{d\Phi}{dr} \right) \right\} \right) \hat{W} \right], \end{aligned} \quad (2.19)$$

$$\begin{aligned} &\left[1 - \frac{3m}{r} - \frac{l(l+1)}{2} - 4\pi r^2 P \right] \hat{H} - 8\pi r^2 e^{-\Phi} \hat{X} \\ &\quad + r^2 e^{-2\Lambda} \left[\omega^2 e^{-2\Phi} - \frac{l(l+1)}{2r} \frac{d\Phi}{dr} \right] \hat{H}_1 \end{aligned}$$

$$- \left[1 + \omega^2 r^2 e^{-2\Phi} - \frac{l(l+1)}{2} - (r - 3m - 4\pi r^3 P) \frac{d\Phi}{dr} \right] \hat{K} = 0, \quad (2.20)$$

$$\hat{V} = \frac{e^{2\Phi}}{\omega^2(P+\rho)} \left[e^{-\Phi} \hat{X} + \frac{1}{r} \frac{dP}{dr} e^{-\Lambda} \hat{W} + \frac{1}{2}(P+\rho) \hat{H} \right], \quad (2.21)$$

where γ is the adiabatic index of the unperturbed stellar model defined by

$$\gamma = \frac{\rho + P}{P} \left(\frac{\partial P}{\partial \rho} \right)_{\text{ad}}. \quad (2.22)$$

Eqs. (2.16)–(2.19) give a set of differential equations for the variables \hat{H}_1 , \hat{K} , \hat{W} and \hat{X} , while Eqs. (2.20) and (2.21) are the algebraic equations for the variables \hat{H} and \hat{V} .

C. the perturbations outside the stars

In the region outside the star, the perturbations are described by the Zerilli equations. Setting $m = M$, $\hat{W} = \hat{V} = 0$, and replacing \hat{H}_1, \hat{K} with new variables Z , dZ/dr_* defined by

$$r^l \hat{K} = \frac{\lambda(\lambda+1)r^2 + 3\lambda M r + 6M^2}{r^2(\lambda r + 3M)} Z + \frac{dZ}{dr_*}, \quad (2.23)$$

$$r^{l+1} \hat{H}_1 = \frac{\lambda r^2 - 3\lambda M r - 3M^2}{(r-2M)(\lambda r + 3M)} Z + \frac{r^2}{r-2M} \frac{dZ}{dr_*}, \quad (2.24)$$

we recover the Zerilli equations. Here r_* is the tortoise coordinates and $\lambda \equiv l(l+1)/2 - 1$.

D. boundary conditions

In order to solve the above perturbation equations, we have to impose the boundary conditions. At the center of the star, we have regularity condition for the perturbative variables. We expand all variables by Taylor power-series near $r = 0$ in a similar way of Detweiler and Lindblom [12] (see Appendix A). Another boundary condition is that the pressure vanishes at the stellar surface. Then the perturbed pressure \hat{X} , ΔP is given by

$$\Delta P = -r^l e^{-\Phi} \hat{X} \quad (2.25)$$

also vanishes there. This boundary condition at the surface of star is equivalent to $\hat{X}(R) = 0$. The last condition is that there exist only outgoing gravitational waves at infinity. We also have a junction condition at the surface of discontinuity, where the variables of $\hat{H}_1, \hat{K}, \hat{W}, \Delta P$ (and then \hat{X}) must be continuous. Note that, \hat{H} and \hat{V} are determined by Eqs. (2.20) and (2.21). \hat{H} is continuous but \hat{V} is discontinuous.

III. NUMERICAL RESULTS

A. models of neutron star

As a concrete example of density discontinuity, we know kaon condensation [2], which may occur at $\rho_{\text{dis}}^{(+)} = 1.466 \times 10^{15} \text{ g/cm}^3$ with the discontinuity $\rho_{\text{dis}}^{(-)}/\rho_{\text{dis}}^{(+)} = 0.414$ for a cold neutron star. Hence we consider density discontinuity around this value, i.e. we study the following three cases: $\rho_{\text{dis}}^{(+)} = 8.0 \times 10^{14}$, 1.2×10^{15} and $1.6 \times 10^{15} \text{ g/cm}^3$. First we briefly discuss a models of a neutron star with density discontinuity. As mentioned before, we have six unknown parameters: $n_{(-)}, K_{(-)}, n_{(+)}, \rho_{\text{dis}}^{(+)}, \rho_{\text{dis}}^{(-)}/\rho_{\text{dis}}^{(+)}$ and ρ_c . We set $n_{(-)} = 1.0$ and $K_{(-)} = 100 \text{ (km}^2\text{)}$, which are usually adopted in a neutron star model. The rest four are $n_{(+)}, \rho_{\text{dis}}^{(+)}, \rho_{\text{dis}}^{(-)}/\rho_{\text{dis}}^{(+)}$ and ρ_c .

First we show the gravitational mass M with respect to a central density ρ_c for several values of $n_{(+)}, \rho_{\text{dis}}^{(+)}, \rho_{\text{dis}}^{(-)}/\rho_{\text{dis}}^{(+)}$ in Figs. 2-4.

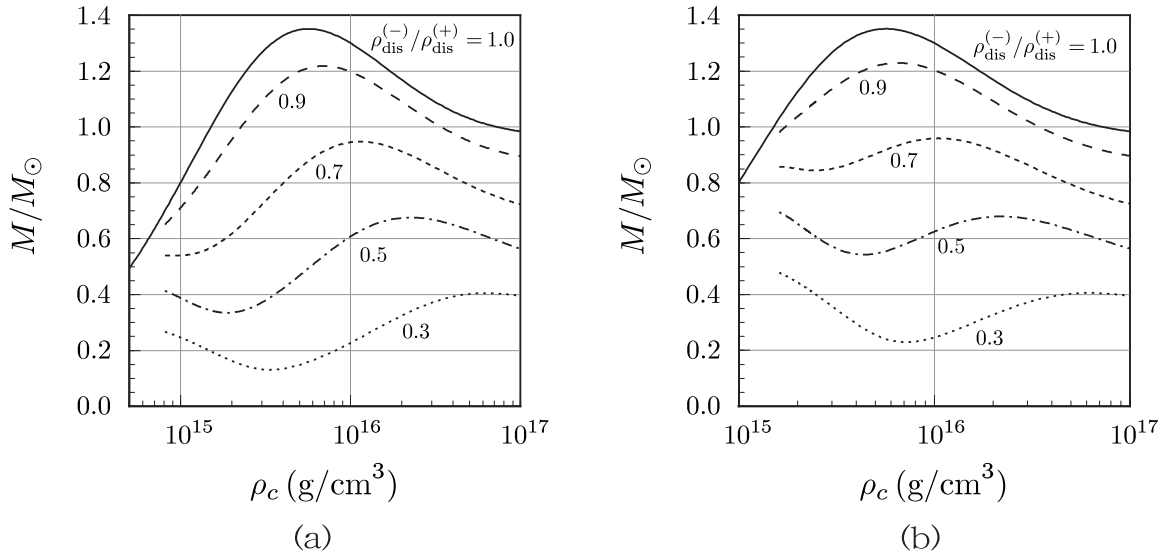


FIG. 2. The relation between the central density ρ_c and the gravitational mass of a neutron star M for $n_{(+)} = 1.0$. Fig. 2(a) is the case of $\rho_{\text{dis}}^{(+)} = 8.0 \times 10^{14}$ (g/cm³), while Fig. 2(b) is the case of $\rho_{\text{dis}}^{(+)} = 1.6 \times 10^{15}$ (g/cm³). The numbers associated with each curve are the values of $\rho_{\text{dis}}^{(-)}/\rho_{\text{dis}}^{(+)}$.

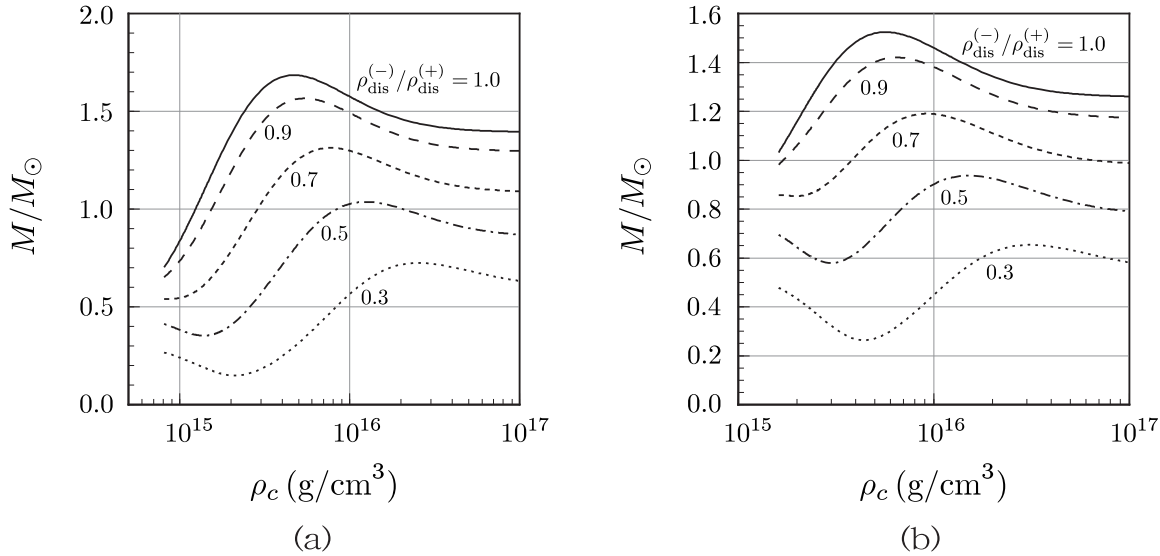


FIG. 3. The same figures as Fig. 2 for the case of $n_{(+)} = 0.7$.

As for inner polytropic index, we set $n_{(+)} = 1.0$ (Fig. 2), 0.7 (Fig. 3), 1.5 (Fig. 4). For each polytropic index, we consider two models with different density at discontinuity: $\rho_{\text{dis}}^{(+)} = 8.0 \times 10^{14}$ (a) and 1.6×10^{15} g/cm³ (b). We depict the M - ρ_c diagram for each value of $\rho_{\text{dis}}^{(-)}/\rho_{\text{dis}}^{(+)} = 1.0$ (no discontinuity), 0.9, 0.7, 0.5, and 0.3. Fig. 2 for $n_{(+)} = 1.0$ shows that the maximum masses for each value of $\rho_{\text{dis}}^{(-)}/\rho_{\text{dis}}^{(+)}$ do not depend on density discontinuity $\rho_{\text{dis}}^{(+)}$. As $\rho_{\text{dis}}^{(-)}/\rho_{\text{dis}}^{(+)}$ gets small, the maximum mass decreases and the stable region ($dM/d\rho_c > 0$) becomes narrower and moves to high density region.

For $n_{(+)} \neq 1.0$, the maximum mass depends on $\rho_{\text{dis}}^{(+)}$. In fact, for $n_{(+)} < 1.0$ (Fig. 3), the maximum mass decreases as $\rho_{\text{dis}}^{(+)}$ increases, while for $n_{(+)} > 1.0$ (Fig. 4), the maximum mass increases. As the equation of state of inner region becomes more stiff, i.e. as $n_{(+)}$ decreases, the maximum mass gets large. The other properties about maximum mass

for $n_{(+)} = 0.7$ and 1.5 are same as those of $n_{(+)} = 1.0$. Note that for the case of $n_{(+)} = 1.5$, all stellar models are unstable if discontinuity gets large.

In what follows, we discuss only stable stellar models, i.e. $dM/d\rho_c > 0$. In our analysis, we fix the mass of a neutron star M ($1.2M_\odot$, $0.5M_\odot$) because M may be determined by other observations. In Table I, Table II and Table III, we summarize the properties of background stellar models.

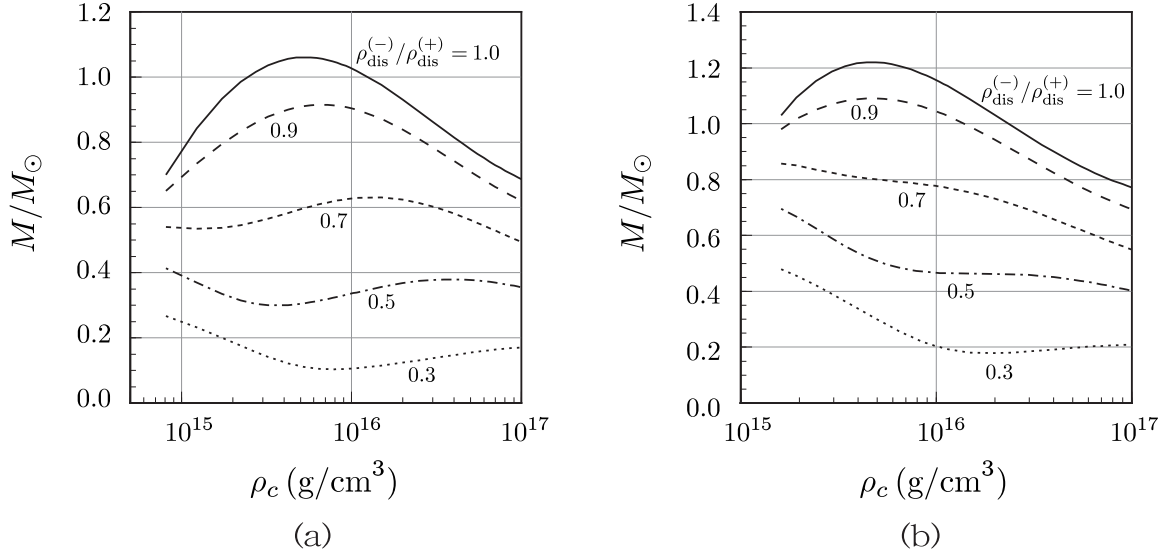


FIG. 4. The same figures as Fig. 2 for the case of $n_{(+)} = 1.5$.

B. Quasi-normal modes for a stellar model without discontinuity

In order to find a specific property in quasi-normal modes of a neutron star with discontinuity, first we calculate of $l = 2$ in the case of a stellar model without discontinuity as reference. In this case, we have to set two parameters; the polytropic index n and polytropic coefficient K , if we fix the total mass M . We adopt the following values; $(n, K) = (1.0, 100\text{km}^2)$, $(1.0, 200\text{km}^2)$, $(1.5, 15\text{km}^4/3)$, $(2.0, 3.5\text{km})$ for $M = 1.2M_\odot$. We also the case of $M = 0.5M_\odot$ with $(n, K) = (1.0, 100\text{km}^2)$ to examine the mass dependence. The properties of the neutron star models are summarized in Table IV.

The quasi-normal modes of the gravitational wave emitted from such stars are plotted in Figure 5 and listed in Table V. The plot point corresponds to the so-called f-mode of each stellar model. In this table we show the mode frequency ω by two normalizations: one is ωM and the other is $\omega(R^3/M)^{1/2}$. Although the f-mode is determined by the radius as well as the mass, we may not know the radius from observation. Then we can plot the data by ωM . In the figure, however, we only show $\omega(R^3/M)^{1/2}$. In a neutron star, we usually find many p-modes as well as f-mode, but we only show the lowest f-mode here because that we are interested in new mode which appears in low frequency for a star with discontinuity.

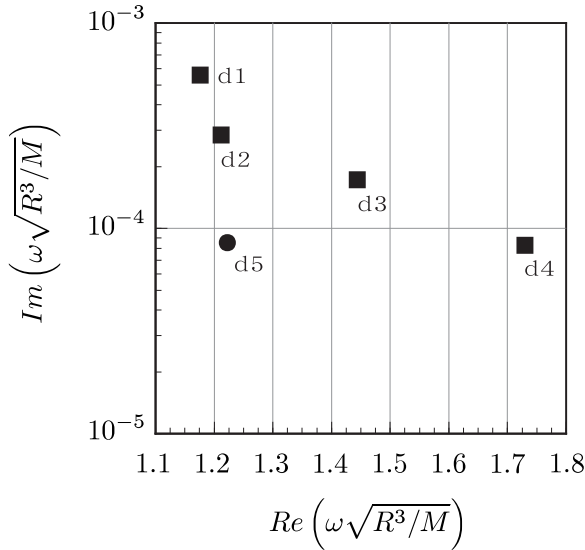


FIG. 5. The quasi normal mode (f-mode) of a neutron star without density discontinuity. The labels associated with each mark correspond to the models in Table IV.

From Fig. 5, we find that the real part of eigenfrequency gets large as equation of state is softer. For example, the frequency in the case 'd4' is by 47% larger than that in the case 'd1'. However, this tendency becomes reverse if we use another normalization (ωM) because the radius of a neutron star constructed by soft matter is larger than one constructed by stiff matter (see Table IV). We also find that the imaginary part of eigenfrequency increases as the stellar mass increases, but the real part is insensitive to the mass.

C. Quasi-normal modes for a stellar model with discontinuity

In the case with discontinuity, we have three unknown parameters: $n_{(+)}$, $\rho_{\text{dis}}^{(+)}$ and $\rho_{\text{dis}}^{(-)}/\rho_{\text{dis}}^{(+)}$. First we show the eigenfrequency of quasi-normal modes of $l = 2$ for the case of $n_{(+)} = 1.0$. We fix the mass of a neutron star as $M = 1.2M_{\odot}$ or $0.5M_{\odot}$. Now two free parameters are $\rho_{\text{dis}}^{(+)}$ and $\rho_{\text{dis}}^{(-)}/\rho_{\text{dis}}^{(+)}$.

We show the f-mode for $M = 1.2M_{\odot}$ and $0.5M_{\odot}$ in Fig. 6. The numerical values are given in Table VI and Table VII.

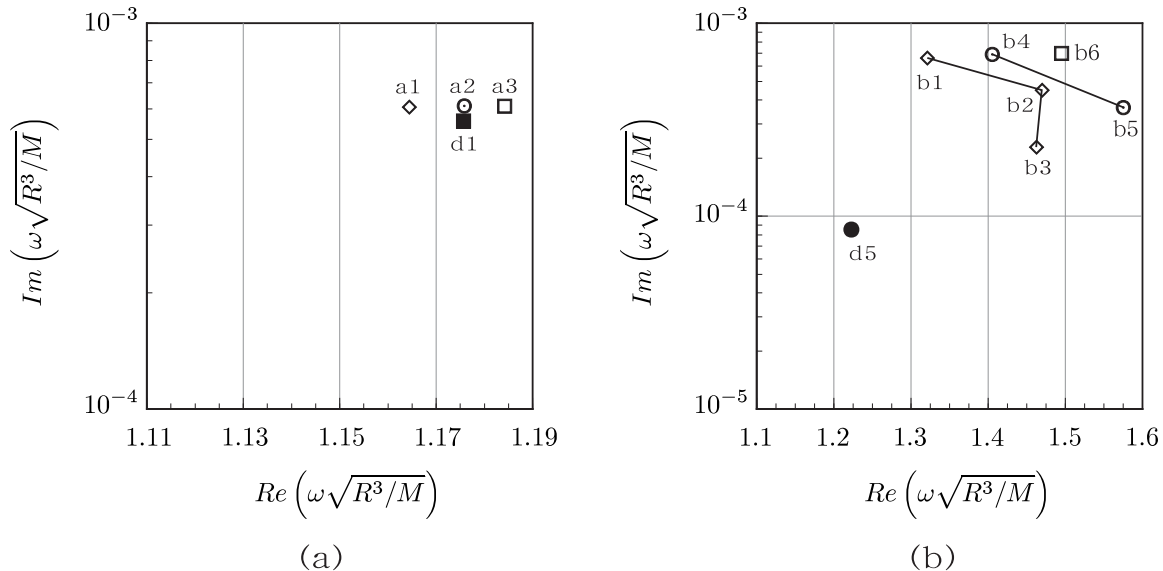


FIG. 6. The quasi normal mode (f-mode) of a neutron star with density discontinuity. We set $n_{(+)} = 1.0$. The left figure (a) shows the result of a star with $M = 1.2M_{\odot}$, while the right one (b) corresponds to a star with $M = 0.5M_{\odot}$. The labels associated with each mark correspond to the models in Table I and in Table II. The data of 'd1' and 'd5', which are the models without discontinuity for $n = 1.0$ and $K = 100 \text{ (km}^2\text{)}$, are also plotted as a reference.

For f-mode, we find that the mode frequency for less massive star ($0.5 M_{\odot}$) is more sensitive to discontinuity than that for massive star ($1.2 M_{\odot}$). For example, the difference of the model 'b5' from the model without discontinuity is larger than 28% for $0.5M_{\odot}$. It is also found that the imaginary part of eigenfrequencies in the model with discontinuity is larger than one without discontinuity, and this difference becomes larger as M/R increases.

The results of g-mode for $M = 1.2M_{\odot}$ and $0.5M_{\odot}$ are given in Fig. 7 and in Table VIII and Table IX. For g-mode, we also find the similar properties to the f-mode. The mode frequency in a less massive star is more sensitive than that in a massive star, in particular the imaginary part changes by the factor $10^2 - 10^4$ for the same $\rho_{\text{dis}}^{(+)}$ depending on the amount of discontinuity (see Fig.7). Furthermore, the existence of g-mode is due to discontinuity, and it turns out that its imaginary part of g-mode is not always so small if the discontinuity is very large. We conclude that the damping rate of g-mode may not be ignored in a particular situation.

Next we calculate the eigenfrequencies of f-mode and g-mode for $n_{(+)} = 0.7$. The results of f-modes and g-mode are shown in Fig. 8(a) with the case of the model without discontinuity, and in Fig. 8(b), respectively. The numerical data are given in Table X and Table XI, respectively. By comparing the upper panel in Fig. 6(a), we find that the effect of change of equation of state is quite small. On the other hand, the imaginary part of g-mode becomes by 10 times larger than the case of $n = 1$ due to the existence of the inner stiff matter. Furthermore, in this case, even if the density is continuous ($\rho_{\text{dis}}^{(-)}/\rho_{\text{dis}}^{(+)} = 1.0$), one may expect the appearance of g-mode because of discontinuity of the equation of state ($n_{(+)} = 0.7$ and $n_{(-)} = 1.0$). However, we could not find g-mode in our calculation. This may be because the g-mode does not exist or is too small to be found.

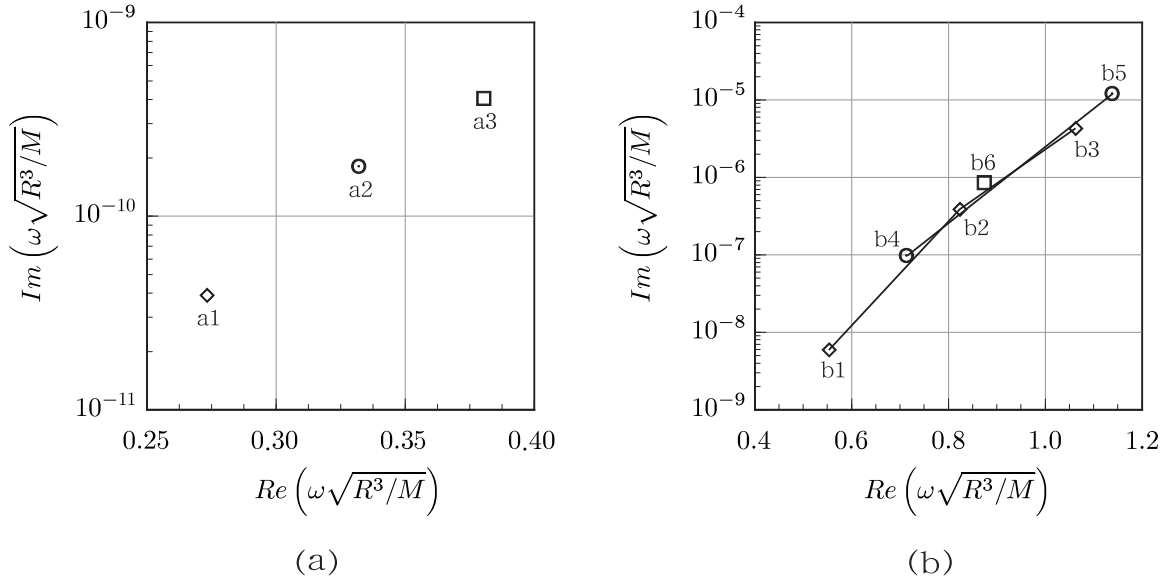


FIG. 7. The quasi normal mode (g-mode) of a neutron star with density discontinuity. The setting is the same as Fig. 6.

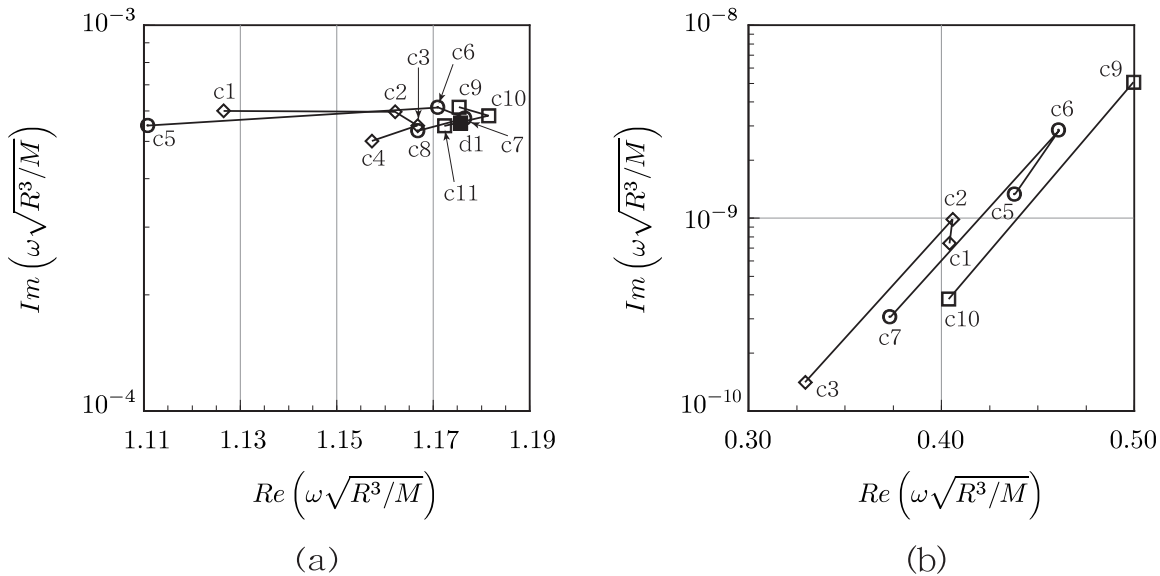


FIG. 8. The quasi normal modes of a neutron star with density discontinuity ((a) f-mode and (b) g-mode). We set $n_{(+)} = 0.7$ and $M = 1.2M_{\odot}$. The labels associated with each mark correspond to the models in Table III. The data of 'd1', which is the model without discontinuity for $n = 1.0$ and $K = 100$ (km²), are also plotted as a reference.

D. Comparison with the Cowling approximation

Finally, by using relativistic Cowling approximation [11], we shall calculate the f- and g-modes, and compare them to our results. In the Cowling approximation, metric perturbation is ignored and only stellar oscillation is taken into account. Hence, the eigenfrequency has only the real part. The result is given in Table XII for $\rho_{(+)} = 8.0 \times 10^{14}$ (g/cm³). The error (the difference from our numerical value) estimated by

$$error = \frac{\omega_{\text{COW}} - \text{Re}(\omega)}{\text{Re}(\omega)}, \quad (3.1)$$

is also shown. Here ω_{COW} is the eigenfrequency found by the Cowling approximation, and $\omega_{\text{COW}}^{(g)}$ and $\omega_{\text{COW}}^{(f)}$ denote those of g- and f-modes, respectively. From Table XII, we find that the Cowling approximation is very accurate for g-mode if $\rho_{(+)}$ is at least in this region, although it is not so good for the f-mode.

IV. CONCLUSION

In this paper we calculate the eigenfrequencies of f-mode and g-mode to examine the dependence of the discontinuity of the density if there exists. We investigate with the various discontinuity, by changing $\rho_{\text{dis}}^{(+)}$ and $\rho_{\text{dis}}^{(-)}/\rho_{\text{dis}}^{(+)}$, for the case that the total mass is fixed $1.2M_{\odot}$ for $n_{(+)} = 1.0$, 0.7 and $0.5M_{\odot}$ for $n_{(+)} = 1.0$. In consequence we find that the dependence of the eigenfrequencies of f-mode on the discontinuity of the density is more strongly for the case that the total mass is smaller. The effect that the inner matter is stiff, $n_{(+)} = 0.7$ and $n_{(-)} = 1.0$, is quite small for f-mode. And it is found that the imaginary part of the eigenfrequencies of g-mode become a little large for the case that inner matter is stiff. In general imaginary part of g-mode is quite small, but we find that in particular situation such that an inner polytropic index is the same as an outer one and total mass is rather small, the imaginary part of g-mode may not be ignored.

For the considering the circumstances mentioned above, it might be possible to judge whether the discontinuity of the density exist or not by the direct observation of the gravitational waves, which might be practicable in future observation, for even f-mode in the particular situation which the total mass is small. Of course, if the gravitational waves of g-mode is directly observed for such stars as the small massive ones, it is found that the discontinuity of the density exist. So we can judge the existence of the phase transition of the density in the neutron stars by the direct

observation of the gravitational waves, though we need to collect the detailed data of the eigenfrequencies for some characteristic mode.

Finally we find also that Cowling approximation is quite accurate for g-mode.

ACKNOWLEDGMENTS

We would like to thank M. Saijo for useful discussion. HS acknowledges T. Harada for valuable comments. This work was supported partially by JSPS Grants-in-Aid (No. 1205705) and by the Waseda University Grant for Special Research Projects.

APPENDIX A: THE TAYLOR EXPANSION AT THE CENTER OF A NEUTRON STAR

Here we present the explicit perturbation equations (2.16)–(2.21) by the expansion at the center of a neutron star. ρ , P and Φ are expanded at $r = 0$ as

$$\rho(r) = \rho^{(0)} + \frac{1}{2}\rho^{(2)}r^2 + O(r^4), \quad (\text{A1})$$

$$P(r) = P^{(0)} + \frac{1}{2}P^{(2)}r^2 + \frac{1}{4}P^{(4)}r^4 + O(r^6), \quad (\text{A2})$$

$$\Phi(r) = \Phi^{(0)} + \frac{1}{2}\Phi^{(2)}r^2 + \frac{1}{4}\Phi^{(4)}r^4 + O(r^6). \quad (\text{A3})$$

where the coefficients are obtained from Eqs. (2.2)–(2.4) and (2.22) as

$$\Phi^{(2)} = \frac{4\pi}{3}\rho^{(0)} + 4\pi P^{(0)}, \quad (\text{A4})$$

$$P^{(2)} = -\left(P^{(0)} + \rho^{(0)}\right)\Phi^{(2)}, \quad (\text{A5})$$

$$\rho^{(2)} = \frac{P^{(0)} + \rho^{(0)}}{P^{(0)}\gamma^{(0)}}P^{(2)}, \quad (\text{A6})$$

$$\Phi^{(4)} = \frac{2\pi}{5}\rho^{(2)} + 2\pi P^{(2)} + \frac{32\pi^2}{9}\rho^{(0)2} + \frac{32\pi^2}{3}\rho^{(0)}P^{(0)}, \quad (\text{A7})$$

$$P^{(4)} = -\left(P^{(0)} + \rho^{(0)}\right)\Phi^{(4)} - \frac{1}{2}\left(P^{(2)} + \rho^{(2)}\right)\Phi^{(2)}. \quad (\text{A8})$$

$\gamma^{(0)}$ is the adiabatic index at $r = 0$, which is defined by the equation of state. The perturbation variables \hat{H}_1 , \hat{K} , \hat{W} and \hat{X} are expanded at $r = 0$ follows,

$$\hat{H}_1(r) = \hat{H}_1^{(0)} + \frac{1}{2}\hat{H}_1^{(2)}r^2 + O(r^4), \quad (\text{A9})$$

$$\hat{K}(r) = \hat{K}^{(0)} + \frac{1}{2}\hat{K}^{(2)}r^2 + O(r^4), \quad (\text{A10})$$

$$\hat{W}(r) = \hat{W}^{(0)} + \frac{1}{2}\hat{W}^{(2)}r^2 + O(r^4), \quad (\text{A11})$$

$$\hat{X}(r) = \hat{X}^{(0)} + \frac{1}{2}\hat{X}^{(2)}r^2 + O(r^4), \quad (\text{A12})$$

where the leading order coefficients in these equations are fixed by the perturbation equations (2.16)–(2.21) as

$$\hat{H}_1^{(0)} = \frac{1}{l(l+1)} \left[2l\hat{K}^{(0)} - 16\pi \left(P^{(0)} + \rho^{(0)} \right) \hat{W}^{(0)} \right], \quad (\text{A13})$$

$$\hat{X}^{(0)} = \left(P^{(0)} + \rho^{(0)} \right) e^{\Phi^{(0)}} \left[-\frac{1}{2}\hat{K}^{(0)} + \left(\frac{4\pi}{3}\rho^{(0)} + 4\pi P^{(0)} - \frac{\omega^2}{l}e^{-2\Phi^{(0)}} \right) \hat{W}^{(0)} \right]. \quad (\text{A14})$$

In the similar way, by using the equations (2.16)–(2.21), we find the second order coefficients in the expansion as

$$\begin{aligned} & \frac{l+3}{2}\hat{H}_1^{(2)} - \hat{K}^{(2)} + 8\pi(P^{(0)} + \rho^{(0)})\frac{l+3}{l(l+1)}\hat{W}^{(2)} \\ &= \left\{ \frac{4\pi}{3}(2l+3) - 4\pi P^{(0)} \right\} \hat{H}_1^{(0)} - \frac{8\pi}{l}(P^{(2)} + \rho^{(2)})\hat{W}^{(0)} + 8\pi(P^{(0)} + \rho^{(0)})Q_1 + \frac{1}{2}Q_0, \end{aligned} \quad (\text{A15})$$

$$\begin{aligned} & \frac{l+2}{2}\hat{K}^{(2)} - \frac{l(l+1)}{4}\hat{H}_1^{(2)} - 4\pi(P^{(0)} + \rho^{(0)})\hat{W}^{(2)} \\ &= 4\pi \left[P^{(2)} + \rho^{(2)} + \frac{8\pi}{3}\rho^{(0)}(P^{(0)} + \rho^{(0)}) \right] \hat{W}^{(0)} + \left(\frac{4\pi}{3}\rho^{(0)} + 4\pi P^{(0)} \right) \hat{K}^{(0)} + \frac{1}{2}Q_0, \end{aligned} \quad (\text{A16})$$

$$e^{\Phi^{(0)}}(P^{(0)} + \rho^{(0)}) \left[\frac{\omega^2}{2}e^{-2\Phi^{(0)}} + 2\pi(P^{(0)} + \rho^{(0)}) - \frac{l+2}{2}\Phi^{(2)} \right] \hat{W}^{(2)}$$

$$\begin{aligned}
& + \frac{l+2}{2} \hat{X}^{(2)} + \frac{l(l+1)}{8} e^{\Phi^{(0)}} (P^{(0)} + \rho^{(0)}) \hat{H}_1^{(2)} \\
= & e^{\Phi^{(0)}} (P^{(0)} + \rho^{(0)}) \left[-\Phi^{(2)} \hat{K}^{(0)} - \frac{1}{4} Q_0 - \frac{\omega^2}{2} e^{-2\Phi^{(0)}} \hat{H}_1^{(0)} - \frac{l(l+1)}{2} \Phi^{(2)} Q_1 \right. \\
& + \left\{ (l+1) \Phi^{(4)} - 2\pi(P^{(2)} + \rho^{(2)}) - \frac{16\pi^2}{3} \rho^{(0)} (P^{(0)} + \rho^{(0)}) - \frac{4\pi}{3} \rho^{(0)} \Phi^{(2)} \right. \\
& \left. \left. + \Phi^{(4)} + \omega^2 e^{-2\Phi^{(0)}} \left(\Phi^{(2)} - \frac{4\pi}{3} \rho^{(0)} \right) \right\} \hat{W}^{(0)} \right] + \frac{l}{2} \left(\Phi^{(2)} + \frac{P^{(2)} + \rho^{(2)}}{P^{(0)} + \rho^{(0)}} \right) \hat{X}^{(0)}, \tag{A17} \\
& - \frac{1}{4} (P^{(0)} + \rho^{(0)}) \hat{K}^{(2)} - \frac{1}{2} \left[P^{(2)} + \frac{l+3}{l(l+1)} \omega^2 e^{-2\Phi^{(0)}} (P^{(0)} + \rho^{(0)}) \right] \hat{W}^{(2)} - \frac{1}{2} e^{-\Phi^{(0)}} \hat{X}^{(2)} \\
= & - \frac{1}{2} e^{-\Phi^{(0)}} \Phi^{(2)} \hat{X}^{(0)} + \frac{1}{4} (P^{(2)} + \rho^{(2)}) \hat{K}^{(0)} + \frac{1}{4} (P^{(0)} + \rho^{(0)}) Q_0 \\
& + \left[P^{(4)} - \frac{4\pi}{3} \rho^{(0)} P^{(2)} + \frac{\omega^2}{l} e^{-2\Phi^{(0)}} \left\{ \frac{1}{2} (P^{(2)} + \rho^{(2)}) - (P^{(0)} + \rho^{(0)}) \Phi^{(2)} \right\} \right] \hat{W}^{(0)} \\
& - \frac{1}{2} \omega^2 e^{-2\Phi^{(0)}} (P^{(0)} + \rho^{(0)}) Q_1, \tag{A18}
\end{aligned}$$

where Q_0 and Q_1 are defined by

$$\begin{aligned}
Q_0 \equiv & \frac{4}{(l+2)(l-1)} \left[-8\pi e^{-\Phi^{(0)}} \hat{X}^{(0)} - \left(\omega^2 e^{-2\Phi^{(0)}} + \frac{8\pi}{3} \rho^{(0)} \right) \hat{K}^{(0)} \right. \\
& \left. + \left\{ \omega^2 e^{-2\Phi^{(0)}} - l(l+1) \left(\frac{2\pi}{3} \rho^{(0)} + 2\pi P^{(0)} \right) \right\} \hat{H}_1^{(0)} \right], \tag{A19}
\end{aligned}$$

$$Q_1 \equiv \frac{2}{l(l+1)} \left[\frac{1}{\gamma^{(0)} P^{(0)}} e^{-\Phi^{(0)}} \hat{X}^{(0)} - \frac{3}{2} \hat{K}^{(0)} + \frac{4\pi(l+1)}{3} \rho^{(0)} \hat{W}^{(0)} \right]. \tag{A20}$$

\hat{H} and \hat{V} are also expanded at $r = 0$ as

$$\hat{H}(r) = \hat{H}^{(0)} + \frac{1}{2} \hat{H}^{(2)} r^2 + O(r^4), \tag{A21}$$

$$\hat{V}(r) = \hat{V}^{(0)} + \frac{1}{2} \hat{V}^{(2)} r^2 + O(r^4), \tag{A22}$$

where the coefficients are given by

$$\hat{H}^{(0)} = \hat{K}^{(0)}, \tag{A23}$$

$$\hat{V}^{(0)} = -\frac{1}{l} \hat{W}^{(0)}, \tag{A24}$$

$$\hat{H}^{(2)} = Q_0 + \hat{K}^{(2)}, \tag{A25}$$

$$\hat{V}^{(2)} = Q_1 - \frac{l+3}{l(l+1)} \hat{W}^{(2)}. \tag{A26}$$

APPENDIX B: HOW TO CALCULATE THE QUASI NORMAL MODES

To calculate the quasi normal modes of a neutron star, we follow the method developed by Leins, Nollert and Soffel [13]. First, we change the variables from Zerilli's one (Z) to the Regge-Wheeler's one (Q), because the effective potential in the Regge-Wheeler equation is very simple. The relation between those two variables given by [14]

$$(\kappa + 2i\omega\beta)Z = (\kappa + 2\beta^2 f(r))Q + 2\beta \frac{dQ}{dr_*}, \quad (\text{B1})$$

$$(\kappa - 2i\omega\beta)Q = (\kappa + 2\beta^2 f(r))Z - 2\beta \frac{dZ}{dr_*}, \quad (\text{B2})$$

where

$$\beta \equiv 6M, \quad (\text{B3})$$

$$\kappa \equiv 4\lambda(\lambda + 1), \quad (\text{B4})$$

$$f(r) \equiv \frac{r - 2M}{2r^2(\lambda r + 3M)}. \quad (\text{B5})$$

To find the solution of the Regge-Wheeler with appropriate boundary condition at infinity, we expand the variable Q at a finite radius $r = r_a$ as

$$Q(r) = \left(\frac{r}{2M} - 1\right)^{-2iM\omega} e^{-i\omega r} \sum_{n=0}^{\infty} a_n \left(1 - \frac{r_a}{r}\right)^n. \quad (\text{B6})$$

By substituting this into the Regge-Wheeler equation, we obtain a four-term recurrence relation for a_n ($n \geq 2$);

$$\alpha_n a_{n+1} + \beta_n a_n + \gamma_n a_{n-1} + \delta_n a_{n-2} = 0, \quad (\text{B7})$$

where

$$\alpha_n = \left(1 - \frac{2M}{r_a}\right) n(n+1), \quad (\text{B8})$$

$$\beta_n = -2 \left\{ i\omega r_a + \left(1 - \frac{3M}{r_a}\right) n \right\} n, \quad (\text{B9})$$

$$\gamma_n = \left(1 - \frac{6M}{r_a}\right) n(n-1) + \frac{6M}{r_a} - l(l+1), \quad (\text{B10})$$

$$\delta_n = \frac{2M}{r_a} (n-3)(n+1). \quad (\text{B11})$$

The coefficients a_{-1} , a_0 , and a_1 are given by the value of Q and dQ/dr at $r = r_a$ as

$$a_{-1} = 0, \quad (\text{B12})$$

$$a_0 = \frac{Q(r_a)}{\chi(r_a)}, \quad (\text{B13})$$

$$a_1 = \frac{r_a}{\chi(r_a)} \left[\frac{dQ(r_a)}{dr} + \frac{i\omega r_a}{r_a - 2M} Q(r_a) \right], \quad (\text{B14})$$

where

$$\chi(r) = \left(\frac{r}{2M} - 1\right)^{-2iM\omega} e^{-i\omega r}. \quad (\text{B15})$$

The convergence condition ($|a_{n+1}/a_n| < 1$) is now $r_a > 4M$ [15]. If $R > 4M$, we set $r_a = R$, while if $R \leq 4M$, we integrate the Regge-Wheeler equation from $r = R$ to $r = r_a (> 4M)$ to find the values of $Q(r_a)$ and $dQ(r_a)/dr$. Furthermore, defining new coefficients $\hat{\alpha}_n$, $\hat{\beta}_n$, and $\hat{\gamma}_n$ as

$$\hat{\alpha}_1 = \alpha_1, \quad \hat{\beta}_1 = \beta_1, \quad \hat{\gamma}_1 = \gamma_1, \quad (\text{B16})$$

and for $n \geq 2$

$$\hat{\alpha}_n = \alpha_n, \quad (\text{B17})$$

$$\hat{\beta}_n = \beta_n - \frac{\hat{\alpha}_{n-1} \delta_n}{\hat{\gamma}_{n-1}}, \quad (\text{B18})$$

$$\hat{\gamma}_n = \gamma_n - \frac{\hat{\beta}_{n-1} \delta_n}{\hat{\gamma}_{n-1}}, \quad (\text{B19})$$

$$\hat{\delta}_n = 0, \quad (\text{B20})$$

the above four-term recurrence relation is reduced into a three-term recurrence relation

$$\hat{\alpha}_n a_{n+1} + \hat{\beta}_n a_n + \hat{\gamma}_n a_{n-1} = 0. \quad (\text{B21})$$

Using this three-term recurrence relation, we find the relation between $\hat{\alpha}_n$, $\hat{\beta}_n$ and $\hat{\gamma}_n$ as the form of continued fraction:

$$\frac{a_1}{a_0} = \frac{-\hat{\gamma}_1}{\hat{\beta}_1 -} \frac{\hat{\alpha}_1 \hat{\gamma}_2}{\hat{\beta}_2 -} \frac{\hat{\alpha}_2 \hat{\gamma}_3}{\hat{\beta}_3 -} \dots, \quad (\text{B22})$$

which can be rewritten as

$$0 = \hat{\beta}_0 - \frac{\hat{\alpha}_0 \hat{\gamma}_1}{\hat{\beta}_1 -} \frac{\hat{\alpha}_1 \hat{\gamma}_2}{\hat{\beta}_2 -} \frac{\hat{\alpha}_2 \hat{\gamma}_3}{\hat{\beta}_3 -} \dots \equiv f(\omega), \quad (\text{B23})$$

where $\hat{\beta}_0 \equiv a_1/a_0$, $\hat{\alpha}_0 \equiv -1$. The eigenfrequency ω of a quasi normal mode is obtained by solving the equation $f(\omega) = 0$.

-
- [1] K. S. Thorne, in *Black Holes and Relativistic Stars*, edited by R. M. Wald (University of Chicago Press, Chicago, 1998), p. 41.
 - [2] T. Tatsumi, and M. Yasuhira, Nucl. Phys. A **670**, 218 (2000).
 - [3] N. Andersson, and K. D. Kokkotas, Phys. Rev. Lett. **77**, 4134 (1996).
 - [4] N. Andersson, and K. D. Kokkotas, Mon. Not. R. Astron. Soc. **299**, 1059 (1998).
 - [5] K. D. Kokkotas, T. A. Apostolatos, and N. Andersson, preprint gr-pc/9901072.
 - [6] P. N. McDermott, Mon. Not. R. Astron. Soc. **245**, 508 (1990).

- [7] L. S. Finn, Mon. Not. R. Astron. Soc. **222**, 393 (1986).
- [8] L. S. Finn, Mon. Not. R. Astron. Soc. **227**, 265 (1987).
- [9] T. G. Cowling, Mon. Not. R. Astron. Soc. **101**, 367 (1941).
- [10] T. E. Strohmayer, Astrophys. J. **417**, 273 (1993).
- [11] P. N. McDermott, H. M. Van Horn and J. F. Scholl Astrophys. J. **268**, 837 (1983).
- [12] L. Lindblom and S. Detweiler, Astrophys. J. Suppl. Ser. **53**, 73 (1983); S. Detweiler and L. Lindblom, Astrophys. J. **292**, 12 (1985).
- [13] M. Leins, H. -P. Nollert, and M. H. Soffel, Phys.Rev.D **48**, 3467 (1993).
- [14] S. Chandrasekhar, in *The Mathematical Theory of Black Holes* (ClarendonPress, Oxford, 1983), chap.4.
- [15] O. Benhar, E. Berti, and V. Ferrari, preprint gr-qc/9901037.

TABLE I. The properties of a neutron star constructed by the equation of state with discontinuity. We set $M = 1.2M_{\odot}$ and $n_{(+)} = 1.0$.

label	$\rho_{\text{dis}}^{(+)} \text{ (g/cm}^3\text{)}$	$\rho_{\text{dis}}^{(-)}/\rho_{\text{dis}}^{(+)}$	$\rho_c \text{ (g/cm}^3\text{)}$	$R \text{ (km)}$	$R_{\text{dis}}/R \text{ (\%)}$	$M_{\text{dis}}/M \text{ (\%)}$	M/R
a1	8.00×10^{14}	0.9	5.017×10^{15}	7.577	81.42	89.23	0.2339
a2	1.20×10^{15}	0.9	4.716×10^{15}	7.800	73.13	78.20	0.2272
a3	1.60×10^{15}	0.9	4.278×10^{15}	8.112	64.02	62.90	0.2184

TABLE II. The properties of a neutron star constructed by the equation of state with discontinuity. We set $M = 0.5M_{\odot}$ and $n_{(+)} = 1.0$.

label	$\rho_{\text{dis}}^{(+)} \text{ (g/cm}^3\text{)}$	$\rho_{\text{dis}}^{(-)}/\rho_{\text{dis}}^{(+)}$	$\rho_c \text{ (g/cm}^3\text{)}$	$R \text{ (km)}$	$R_{\text{dis}}/R \text{ (\%)}$	$M_{\text{dis}}/M \text{ (\%)}$	M/R
b1	8.00×10^{14}	0.4	1.759×10^{16}	3.925	86.99	98.76	0.1881
b2	8.00×10^{14}	0.5	5.800×10^{15}	6.050	73.65	91.10	0.1220
b3	8.00×10^{14}	0.6	2.484×10^{15}	8.465	56.76	65.25	0.08721
b4	1.20×10^{15}	0.4	1.733×10^{16}	4.137	80.71	97.16	0.1785
b5	1.20×10^{15}	0.5	5.127×10^{15}	6.985	59.38	76.64	0.1057
b6	1.60×10^{15}	0.4	1.680×10^{16}	4.407	74.28	94.69	0.1675

TABLE III. The properties of a neutron star constructed by the equation of state with discontinuity. We set $M = 1.2M_{\odot}$ and $n_{(+)} = 0.7$.

label	$\rho_{\text{dis}}^{(+)} \text{ (g/cm}^3\text{)}$	$\rho_{\text{dis}}^{(-)}/\rho_g^{(+)}$	$\rho_c \text{ (g/cm}^3\text{)}$	$R \text{ (km)}$	$R_{\text{dis}}/R \text{ (\%)}$	$M_{\text{dis}}/M \text{ (\%)}$	M/R
c1	8.00×10^{14}	0.7	4.237×10^{15}	7.351	85.64	93.61	0.2410
c2	8.00×10^{14}	0.8	2.787×10^{15}	8.488	79.57	85.53	0.2088
c3	8.00×10^{14}	0.9	2.029×10^{15}	9.387	73.47	74.03	0.1888
c4	8.00×10^{14}	1.0	1.580×10^{15}	10.04	67.38	60.31	0.1765
c5	1.20×10^{15}	0.7	5.924×10^{15}	6.724	83.11	91.86	0.2635
c6	1.20×10^{15}	0.8	3.483×10^{15}	8.090	73.88	78.54	0.2190
c7	1.20×10^{15}	0.9	2.449×10^{15}	9.046	65.08	60.68	0.1959
c8	1.20×10^{15}	1.0	1.903×10^{15}	9.634	56.62	42.14	0.1839
c9	1.60×10^{15}	0.8	4.068×10^{15}	7.862	68.95	71.75	0.2254
c10	1.60×10^{15}	0.9	2.740×10^{15}	8.912	56.79	46.69	0.1988
c11	1.60×10^{15}	1.0	2.146×10^{15}	9.421	45.71	25.46	0.1881

TABLE IV. The properties of a neutron star constructed by the equation of state without discontinuity. The total mass M is fixed $1.2M_{\odot}$ or $0.5M_{\odot}$.

label	Mass (M_{\odot})	n	K	$\rho_c \text{ (g/cm}^3\text{)}$	$R \text{ (km)}$	M/R
d1	1.2	1.0	100 (km^2)	2.427×10^{15}	9.296	0.1906
d2	1.2	1.0	200 (km^2)	5.507×10^{14}	15.10	0.1173
d3	1.2	1.5	15 ($\text{km}^{4/3}$)	2.691×10^{14}	23.49	0.07542
d4	1.2	2.0	3.5 (km)	1.153×10^{14}	38.79	0.04568
d5	0.5	1.0	100 (km^2)	5.067×10^{14}	11.57	0.06384

TABLE V. The numerical data of quasi normal mode (f-mode) of the models in TableIV. These data are plotted in Fig.5 .

label	$\mathcal{R}e(\omega M)$	$\mathcal{I}m(\omega M)$	$\mathcal{R}e\left(\omega\sqrt{R^3/M}\right)$	$\mathcal{I}m\left(\omega\sqrt{R^3/M}\right)$
d1	0.09784	4.643×10^{-5}	1.176	5.579×10^{-4}
d2	0.04869	1.145×10^{-5}	1.211	2.849×10^{-4}
d3	0.02990	3.572×10^{-6}	1.443	1.725×10^{-4}
d4	0.01688	8.075×10^{-7}	1.729	8.270×10^{-5}
d5	0.01974	1.374×10^{-6}	1.224	8.517×10^{-5}

TABLE VI. The numerical data of quasi normal mode (f-mode) of the models in TableI ($M = 1.2M_\odot$ and $n_{(+)} = 1.0$). These data are plotted in Fig.6 (a).

label	$\mathcal{R}e(\omega M)$	$\mathcal{I}m(\omega M)$	$\mathcal{R}e\left(\omega\sqrt{R^3/M}\right)$	$\mathcal{I}m\left(\omega\sqrt{R^3/M}\right)$
a1	0.1317	6.856×10^{-5}	1.164	6.062×10^{-4}
a2	0.1273	6.604×10^{-5}	1.176	6.098×10^{-4}
a3	0.1209	6.221×10^{-5}	1.184	6.093×10^{-4}

TABLE VII. The numerical data of quasi normal mode (f-mode) of the models in TableII ($M = 0.5M_\odot$ and $n_{(+)} = 1.0$). These data are plotted in Fig.6 (b).

label	$\mathcal{R}e(\omega M)$	$\mathcal{I}m(\omega M)$	$\mathcal{R}e\left(\omega\sqrt{R^3/M}\right)$	$\mathcal{I}m\left(\omega\sqrt{R^3/M}\right)$
b1	0.1078	5.384×10^{-5}	1.321	6.600×10^{-4}
b2	0.06266	1.916×10^{-5}	1.470	4.495×10^{-4}
b3	0.03767	5.867×10^{-6}	1.462	2.278×10^{-4}
b4	0.1060	5.185×10^{-5}	1.406	6.878×10^{-4}
b5	0.05416	1.253×10^{-5}	1.576	3.645×10^{-4}
b6	0.1025	4.780×10^{-5}	1.495	6.971×10^{-4}

TABLE VIII. The numerical data of quasi normal mode (g-mode) of the models in TableI ($M = 1.2M_\odot$ and $n_{(+)} = 1.0$). These data are plotted in Fig.7 (a).

label	$\mathcal{R}e(\omega M)$	$\mathcal{I}m(\omega M)$	$\mathcal{R}e\left(\omega\sqrt{R^3/M}\right)$	$\mathcal{I}m\left(\omega\sqrt{R^3/M}\right)$
a1	3.090×10^{-2}	4.410×10^{-12}	0.2732	3.899×10^{-11}
a2	3.598×10^{-2}	1.955×10^{-11}	0.3322	1.806×10^{-10}
a3	3.884×10^{-2}	4.137×10^{-11}	0.3804	4.052×10^{-10}

TABLE IX. The numerical data of quasi normal mode (g-mode) of the models in TableII ($M = 0.5M_{\odot}$ and $n_{(+)} = 1.0$). These data are plotted in Fig.7 (b).

label	$Re(\omega M)$	$Im(\omega M)$	$Re(\omega\sqrt{R^3/M})$	$Im(\omega\sqrt{R^3/M})$
b1	4.514×10^{-2}	4.849×10^{-10}	0.5532	5.944×10^{-9}
b2	3.510×10^{-2}	1.650×10^{-8}	0.8234	3.870×10^{-7}
b3	2.737×10^{-2}	1.104×10^{-7}	1.062	4.287×10^{-6}
b4	5.387×10^{-2}	7.374×10^{-9}	0.7145	9.781×10^{-8}
b5	3.916×10^{-2}	4.150×10^{-7}	1.139	1.208×10^{-5}
b6	5.992×10^{-2}	5.865×10^{-8}	0.8738	8.553×10^{-7}

TABLE X. The numerical data of quasi normal mode (f-mode) of the models in TableIII ($M = 1.2M_{\odot}$ and $n_{(+)} = 0.7$). These data are plotted in Fig.8 (a).

label	$Re(\omega M)$	$Im(\omega M)$	$Re(\omega\sqrt{R^3/M})$	$Im(\omega\sqrt{R^3/M})$
c1	0.1333	7.102×10^{-5}	1.126	6.001×10^{-4}
c2	0.1108	5.692×10^{-5}	1.162	5.967×10^{-4}
c3	0.09569	4.503×10^{-5}	1.167	5.490×10^{-4}
c4	0.08579	3.713×10^{-5}	1.157	5.008×10^{-4}
c5	0.1503	7.432×10^{-5}	1.111	5.494×10^{-4}
c6	0.1200	6.278×10^{-5}	1.171	6.125×10^{-4}
c7	0.1020	4.975×10^{-5}	1.177	5.739×10^{-4}
c8	0.09205	4.201×10^{-5}	1.167	5.326×10^{-4}
c9	0.1258	6.560×10^{-5}	1.175	6.130×10^{-4}
c10	0.1047	5.163×10^{-5}	1.181	5.824×10^{-4}
c11	0.09564	4.476×10^{-5}	1.172	5.487×10^{-4}

TABLE XI. The numerical data of quasi normal mode (g-mode) of the models in TableIII ($M = 1.2M_{\odot}$ and $n_{(+)} = 0.7$). These data are plotted in Fig.8 (b).

label	$Re(\omega M)$	$Im(\omega M)$	$Re(\omega\sqrt{R^3/M})$	$Im(\omega\sqrt{R^3/M})$
c1	4.782×10^{-2}	8.763×10^{-11}	0.4040	7.404×10^{-10}
c2	3.870×10^{-2}	9.396×10^{-11}	0.4057	9.851×10^{-10}
c3	2.701×10^{-2}	1.154×10^{-11}	0.3293	1.407×10^{-10}
c5	5.926×10^{-2}	1.799×10^{-10}	0.4381	1.330×10^{-9}
c6	4.725×10^{-2}	2.931×10^{-10}	0.4610	2.859×10^{-9}
c7	3.238×10^{-2}	2.666×10^{-11}	0.3735	3.075×10^{-10}
c9	5.346×10^{-2}	5.412×10^{-10}	0.4996	5.058×10^{-9}
c10	3.578×10^{-2}	3.374×10^{-11}	0.4036	3.805×10^{-10}

TABLE XII. Comparison with the results of Cowling approximation. The labels in the table corresponds to each model. The data in this Table is only for $\rho_{(+)} = 8.0 \times 10^{14}$ (g/cm³).

label	$\omega_{\text{Cow}}^{(g)} \sqrt{R^3/M}$	$error^{(g)} (\%)$	$\omega_{\text{Cow}}^{(f)} \sqrt{R^3/M}$	$error^{(f)} (\%)$
a1	0.2689	-1.570	1.304	12.01
b1	0.5533	0.01808	1.520	15.10
b2	0.8329	1.161	1.733	17.94
b3	1.107	4.216	1.717	17.41
c1	0.4015	-0.6188	1.291	14.63
c2	0.4016	-1.003	1.355	16.57
c3	0.3232	-1.837	1.379	18.21
c4	---	---	1.388	19.97